DEVELOPMENT AND HEMOSTATIC EVALUATION OF OXIDIZED REGENERATED CELLULOSE DIALDEHYDE CROSSLINKED CHITOSAN PARTICLES

OĞUZ SOGUT[*,**] and UMRAN AYDEMIR SEZER[*,***,****]

[*]*Suleyman Demirel University, Faculty of Medicine, Department of Pharmacology, Medicine, Medical Device and Dermo-cosmetic Research and Application Laboratory-IDAL, 32260, Isparta, Turkey*
[**]*Suleyman Demirel University, Natural Products Application and Research Center, 32200, Isparta, Turkey*
[***]*Suleyman Demirel University, Institute of Health Sciences, Department of Regenerative Medicine, 32200, Isparta, Turkey*
[****]*Semical Technology Industry and Trade Co. Ltd., Suleyman Demirel University Lake District Technopark, 32260, Isparta, Turkey*
✉ *Corresponding author: U. Aydemir Sezer, umransezer@sdu.edu.tr*

Received March 25, 2026

Excessive hemorrhage poses a significant risk, necessitating the development of effective hemostatic agents. However, commercially available products often suffer from poor biocompatibility and biodegradability. This study presented a composite particle material combining water-soluble oxidized regenerated cellulose dialdehyde (ORCdial) and chitosan to enhance hemostatic efficacy and biocompatibility. It was hypothesized that ORCdial formed a gel upon blood contact, while chitosan interacted with the coagulation cascade, making them promising candidates for hemostasis. Particles were synthesized by blending ORCdial and chitosan, lyophilizing, neutralizing, and milling the mixture into particles. Crosslinking was confirmed by FTIR (C=N band at ~1640–1655 cm^{-1}) and solid-state ^{13}C CP/MAS NMR (imine carbon at ~165–170 ppm). Their physicochemical properties and hemostatic performance were evaluated *in vitro*. *In vitro* studies demonstrated that ORCdial-chitosan composites significantly improved clotting efficiency and cell compatibility compared to the commercial hemostatic agent Celox®, with performance varying based on ORCdial content. In conclusion, this study presented a novel, biocompatible, and effective hemostatic material with promising *in vitro* hemostatic performance, offering a potential candidate for further pre-clinical investigation in hemorrhage control.

Keywords: hemostasis, oxidized regenerated cellulose dialdehyde, chitosan, hemostatic agents, excessive hemorrhage

INTRODUCTION

Hemostasis is the complex physiological mechanism through which the body stops bleeding while maintaining blood vessel integrity, and it entails a sequence of precisely controlled actions that work in tandem to produce a blood clot at the site of damage and avoid excessive blood loss.[1] Hemostasis is a crucial physiological mechanism that prevents excessive blood loss and maintains blood vessel integrity and it involves a series of precisely controlled actions that lead to the formation of a blood clot at the site of injury.[1] The trauma and loss of blood in large quantities within a short span of time possess a great risk, thereby causing hypothermia, acidosis, and coagulopathy.[2,3] The blood coagulation mechanism can treat the small wounds intrinsically; however, for severe bleeding and large or complex wounds, hemostatic agents are required to reduce blood loss and eventually death rate.[4]

Various biomaterials and technologies have been developed to manage bleeding, especially in the case of severe external trauma, by using various hemostatic materials including powders, adhesives, hydrogels, and tourniquets that are easy to use, cost-effective, suitable for long-term storage, biodegradable, and do not show side effects, such as thrombosis.[5,6] For instance, Quickclot® is an FDA-approved commercial product made of zeolite for hemostatic purposes, which is in the form of powder, providing practical application. However, these materials still have numerous limitations

during blood absorption, such as necrosis in the skin muscle nerves and temperature sensitivity of veins and tissues around the wound.[7]

Polysaccharides exhibit excellent biocompatibility, making them attractive alternatives to synthetic hemostatic materials. Among polysaccharides, chitosan has been widely utilized as a hemostatic agent due to its film forming ability, antimicrobial properties, and supportive properties on tissue regeneration. Chitosan is considered to interfere with negative ions of blood membranes and promotes blood clotting by allowing the swelling thrombocytes and blood coagulation factors to stick to tissues after absorbing and activating them.[8–10] Even though WoundStat®, Celox®, and HemCon® are commercially available and successful chitosan-based products, each product has its limitations such as inability to stop bleeding quickly due to a low impact rate on the bleeding site; ineffectiveness in controlling excessive bleeding, restrictions on the use of inflammatory responses in tissues around the wound.[11] However, the application of such materials can be widened by combining with other biopolymers or using cross-linking macromolecules. Cross-linking provides a strong connection between chains and the stability that is required for biomedical applications, including hemostasis, scaffolds for cell proliferation.[12]

Oxidized regenerated cellulose (ORC) has been used in clinical applications for many years due to its antibacterial and hemostatic effect.[13] Even though ORC can absorb more liquid than its own mass,[14] its use in hemostatic applications is restricted because of its acidic character, requiring to be removed after the application.[15] The combination of ORC and chitosan may help to obtain effective hemostatic agents with improved properties for biomedical applications. For instance, Cheng *et al.*[16] modified ORC with N,O-carboxymethyl chitosan (N,O-CS), which could form a gel by absorbing blood or have the ability to prevent blood leaks from the veins. Water soluble chitosan was also used for improvement of hemostatic and antibacterial performances of ORC gauze.[17]. ORC-based composites can be obtained by reducing the size of ORC particles physically or by coating the ORC material with chitosan gel. In our previous study, a water-soluble salt form of ORC has been synthesized and investigated for hemostatic efficiency.[18]

ORC based hemostatic products have restrictions because of lack of biocompatibility and insolubility, while chitosan has limited biomedical applications because of lower effectiveness when compared to synthetic hemostatic materials.[13,19] Considering the issues mentioned above, combining these two materials via crosslinking may result in more effective materials and may provide a reference for an optimized oxidized cellulose product for hemostatic applications. To the best of our knowledge, even though the use of dialdehyde-based cross-linkers for chitosan has been widely studied, there is no information about the combination of synthesized ORC dialdehyde (ORCdial) with chitosan.

The development of a novel composite material comprising ORCdial and chitosan offers a promising avenue for hemostatic applications. This study aims to investigate whether the combination of ORCdial and chitosan may improve biocompatibility and hemostatic efficacy, as this composite approach holds potential as a candidate material for the management of excessive hemorrhage.

In this study, chitosan was crosslinked with ORCdial in varying ratios and the hemostatic efficiency was determined to understand the role of the ratio in the Chitosan-ORCdial combination for obtaining both more efficient hemostatic performance and biocompatibility. The results of this study may open a route for a new derivative of ORC and new hemostatic materials by using this derivative as crosslinking agent, aiming at advancing the development of improved hemostatic agents.

EXPERIMENTAL

Materials

Chitosan was purchased from Merck (M_w = 100.000–300.000 Da, Germany). Celox® was obtained from Amazon (www.amazon.com). Regenerated cellulose knitted fabric was obtained from Altaylar Medikal Ltd. Şti. (Ankara, Turkey). Phosphate buffer solution (PBS) tablets, 1 N sodium hydroxide solution (NaOH) and acetone were purchased from Sigma Aldrich (USA).

Sodium hydroxide anhydrous (reagent grade, ≥98%, pellets), sodium (meta)periodate (ACS reagent, reag. Ph. Eur., ≥99.8%), ethanol 96% (EMSURE® Reag. Ph. Eur.), acetone (Puriss. P.A., ACS reagent, reag. ISO, reag. Ph. Eur., ≥99.5%), hydrochloric acid fuming 37% (for analysis EMSURE® ACS, ISO, Reag. Ph. Eur.) were also purchased from Sigma Aldrich (Germany). For flow cytometric analysis, Anti-CD42B, anti-CD62P, anti-CD41 and anti-CD63 antibodies were purchased from Biolegend, San Diego, USA. BD Vacutainer Plus Citrate Tubes 2.7 mL were purchased from BD Biosciences, USA. $CaCI_2.2H_2O$, Dulbecco's Phosphate Buffer Saline (DPBS)

paraformaldehyde, Corning® and Co®96-well tissue culture plates, and TOX-1 3-(4,5-dimethylthiazol-2-yl)-2,5-diphenyltetrazolium bromide (MTT) kit were all purchased from Sigma Aldrich, Germany.

Synthesis of ORC dialdehyde

To synthesize oxidized regenerated cellulose (ORC), regenerated cellulose samples were cut and placed in a stainless steel oxidation chamber. Nitrogen gas was introduced into the chamber for the reaction system and washed with deionized water. The resulting ORC was dissolved in a 0.5 M NaOH solution until the solution became clear with stirring, and ethanol was added to precipitate the ionic form of ORC. The solid material was collected by filtration and washed with acetone prior to drying.[13] To synthesize ORC dialdehyde, ORC fabrics were used as the starting material. 10 g of ORC was dissolved in 100 mL of 0.5 M NaOH, which converted the ORC to NaORC. The reaction mixture was precipitated using 500 mL of ethanol under vacuum and dried in an oven at 45 °C. 10 g of NaORC was dissolved in 200 mL of ultrapure water, and 11.1 g of $NaIO_4$ dissolved in 100 mL was added. The reaction mixture temperature was set to 35 °C, and the pH was adjusted to 3 with 0.1 N HCl. The reaction was incubated in the dark for 4 h. At the end of the reaction, the product was precipitated with ethanol under vacuum, washed 3 times with acetone, and dried under vacuum at room temperature.

Preparation of Chit-ORC dialdehyde particles

Chitosan solutions containing different amounts of ORC dialdehyde (1%, 5%, 10%, 25%, and 50% w/w) were prepared in acetic acid solution (1% v/v). The solutions were poured into well plates and frozen at −20 °C, then lyophilized for 48 h using a freeze-dryer (LD, Christ, UK) (first lyophilization) to establish the porous sponge architecture with intact Schiff base crosslinks. The lyophilized sponges were then immersed in 1 M NaOH solution to neutralize residual acetic acid and adjust the pH of the matrix to alkaline conditions, followed by extensive washing with ultrapure water. The neutralized, water-saturated sponges were lyophilized again for 48 h using the same procedure (second lyophilization) to restore the dry porous structure prior to mechanical milling. The use of 1 M NaOH ensured complete neutralization throughout the sponge volume, and the alkaline pH (pH > 12) was favorable for Schiff base stability, as protonation of the imine nitrogen, which would promote hydrolysis, is suppressed under basic conditions. The dried sponges were milled using a planetary ball mill (Pulverisette 14, Fritsch, Germany) with ten zirconia grinding balls in 10 mm diameter to obtain particles. Milling was performed at a constant temperature of 30 °C at 1200 rpm rotational speed for 8 min. Chitosan sponges without ORC dialdehyde content were prepared to be used as positive control group using the same procedure. Besides, Celox®, a commercial product, was also used as negative control for comparison. Table 1 summarizes the hemostatic materials developed in this study.

Table 1
Hemostatic materials prepared in this study

Materials	Content
Chit-ORCDial1	ORC dialdeyhde cross-linked chitosan (1%, w/w, ORCDial/Chit)
Chit-ORCDial5	ORC dialdeyhde cross-linked chitosan (5%, w/w, ORCDial/Chit)
Chit-ORCDial10	ORC dialdeyhde cross-linked chitosan (10%, w/w, ORCDial/Chit)
Chit-ORCDial25	ORC dialdeyhde cross-linked chitosan (25%, w/w, ORCDial/Chit)
Chit-ORCDial50	ORC dialdehyde cross-linked chitosan (50%, w/w, ORCDial/Chit)
ORCDial	ORC dialdeyhde (100%, w/w, ORCDial)
Chit-ORCDial0	Chitosan (0% w/w, ORCDial)

Characterization of hemostatic materials

The morphology of the prepared samples was characterized using a scanning electron microscope (SEM, JSM-6400, JEOL, USA). Before analysis, the samples were coated with Au-Pd. Fourier transform infrared (FTIR) spectrophotometry (Perkin Elmer, USA) was used to determine the chemical structure of the samples. Attenuated total reflectance (ATR) spectra were obtained using an ATR apparatus with a range of 600-4000 cm^{-1} and a resolution of 4 cm^{-1}. In addition, a high-power solid-state 300 MHz NMR spectrometer (Bruker, Superconducting FT-NMR Spectrometer AvanceTM, with 300 MHz Wide Board Magnet, Germany) was used to perform ^{13}C CPMAS analysis at a spin rate of 8000 Hz with a scan number of 20000. The same amount of sample was used in all analyses.

Measurement of whole blood clotting time

The clotting time of the hemostatic material was evaluated according to the method described by Gaharwar *et al*. To do this, 2 mL of blood was drawn from five healthy volunteers and placed into tubes containing sodium citrate. 0.003 g of the hemostatic material was placed into a 96-well culture plate. 50 µL of whole blood was

added to each sample and coagulation was initiated by the addition of 5 µL of 0.1 M $CaCl_2$. Each study was repeated three times for each material, and thrombus formation was observed by two independent observers.[20]

Platelet activation

Platelet activation was evaluated using the no wash-no lyse method. 2 mL of blood was drawn from four healthy volunteers into sodium citrate tubes (Becton Dickinson, USA). 0.006 g of powder samples were placed in Eppendorf tubes and mixed with 300 µL of DPBS (Dulbecco's Phosphate Buffered Saline). 100 µL of whole blood was added to the powder-DPBS suspension, and platelet activation was terminated by adding 500 µL of fixative solution (1% paraformaldehyde) and incubating at 4 °C for 2 h. Samples were filtered through a cell strainer with a 40 µm pore size, followed by staining with CD62P-FITC, CD42b-PE, CD41-PE Cy5.5, and CD63-PerCp Cy7 antibodies by incubating at room temperature for 15 min. Cells were analyzed using a Beckman Coulter FC500 flow cytometry system (Beckman Coulter, USA). Platelets and platelet-leukocyte aggregates were gated on a Side Scatter/CD41 plot. CXP Analysis software (Beckman Coulter, USA) was used for list mode data analysis.

***In vitro* cell culture studies**

The HUVEC cell line (ATCC CRL-1730) was used to assess the *in vitro* cytotoxicity of the samples. Cells were cultured in DMEM/F12 culture medium supplemented with 10% fetal bovine serum and 1% penicillin-streptomycin antibiotic solution. 5000 cells per well were seeded into a 96-well tissue culture plate in triplicates and incubated overnight for attachment. 0.0003 g of the powder, which was sterilized by UV exposure for 2 h, was added to each well. Healthy cells were used as the positive control, and culture media was used as the negative control. Cellular viability was detected using the TOX-1 MTT-based cytotoxicity kit (Sigma Aldrich) by measuring absorbance at 570 nm using an Epoch Microplate reader (BioTek Instruments Inc., USA) on the 6^{th} and 12^{th} hours after contact with the hemostatic material.

Fluorescence imaging of viability

The viability of cells incubated with powders was evaluated with LIVE/DEAD® Viability/Cytotoxicity Kit (Thermo Fisher Scientific, USA). This kit contains a viability indicator, Calcein AM, which provides a green signal after being cleaved via esterases only present in viable cells and Ethidium Homodimer-1, a fluorescent dye that cannot enter healthy cells, but binds to nucleic materials of cells with compromised membranes to give a red signal. For fluorescent imaging, HUVECs were seeded into a 24 well culture plate as 20.000 cell per well and cultured overnight. 0.001 g pre-sterilized powders, mixed with 500 µL complete culture medium were added to each well and incubated for 72 h. Medium containing powders was removed, cells were washed twice with DPBS and stained with Calcein-AM and Ethidium Homodimer-1 containing DPBS by incubating at room temperature for 45 min. Cells were washed twice after discarding the staining solution and fresh DPBS was added on cells. Fluorescent images were taken via Zeiss Axio Imager 1A at 10X zoom.

Statistical analysis

IBM SPSS Statistics 22 (IBM SPSS, Turkey) was used for all statistical analyses. Prior to inferential testing, the normality of each dataset was assessed using the Shapiro-Wilk test. For datasets that did not follow a normal distribution, the Kruskal-Wallis test was applied for multi-group comparisons, and pairwise post-hoc differences were evaluated using the Mann-Whitney U test with Bonferroni correction. For MTT absorbance data, which met the assumption of normality (Shapiro-Wilk, $p > 0.05$), one-way ANOVA followed by Tukey's Honestly Significant Difference (HSD) post-hoc test was employed to compare group means. This distinction in statistical approach across test types reflects the differing distributional characteristics of the respective datasets. For platelet activation markers, a multiple pairwise t-test with Bonferroni correction was applied to control the family-wise error rate. A significance threshold of $p < 0.05$ was used throughout.

RESULTS AND DISCUSSION

Characteristics of hemostatic materials

The characteristics of hemostatic materials were determined using SEM (Fig. 1a-f), FTIR (Fig. 1g-h), and NMR (Fig. 1i) to observe the porous and rough structure for blood entrapment, to identify active functional groups for cellular binding, and to verify the degree of modification of the molecular architecture.

The SEM micrographs of the lyophilized sponges (Fig. 1a-f) showed a morphological transition from a relatively smooth, dense, and sheet-like surface in the initial samples to an irregular, porous, and fibrous architecture as the concentration of the modified component increased. These structural changes might be characterized by an increase in surface roughness and the formation of an interconnected, fluffy micro-network. This behavior could provide an advantage for hemostatic

applications as it facilitated a higher surface-area-to-volume ratio for blood absorption. The development of fine, fiber-like structures in samples Figure 1d–f was found to be most similar to natural extracellular matrix, potentially enhancing the physical entrapment of red blood cells and accelerating the mechanical stabilization of the fibrin clot. It should be noted that these SEM images represent the internal microstructure of the sponges prior to mechanical milling; the subsequent milling step produced particles of irregular morphology. A systematic characterization of post-milling particle size and morphology remains as a direction for future work.

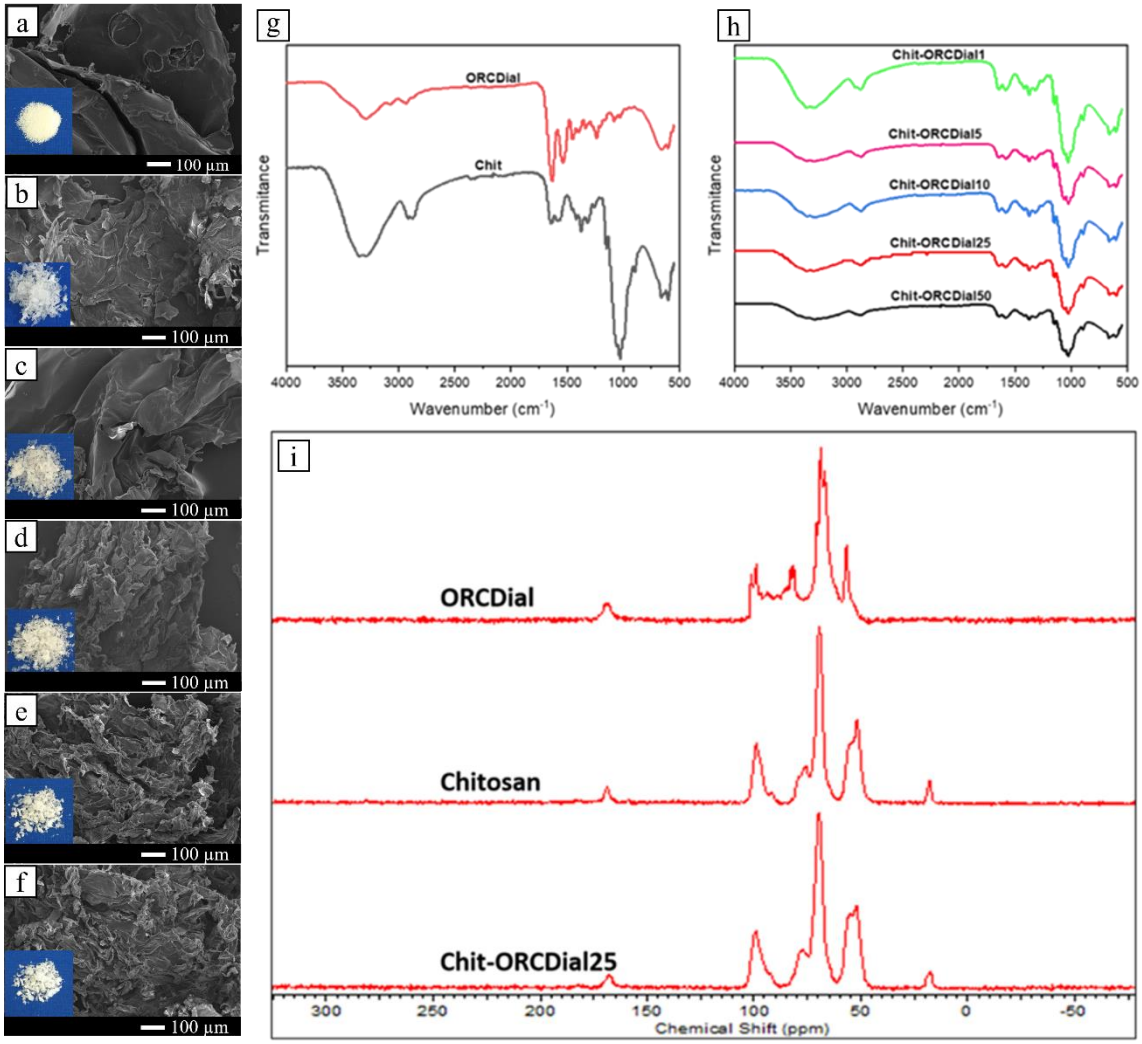

Figure 1: Morphological and chemical characterization of hemostatic materials; (a–f) SEM micrographs of lyophilized sponges showing the microstructural evolution with increasing ORCdial content: (a) Chit-ORCdial0, (b) Chit-ORCdial1, (c) Chit-ORCdial5, (d) Chit-ORCdial10, (e) Chit-ORCdial25, (f) Chit-ORCdial50; (g–h) FTIR spectra confirming Schiff base crosslink formation: (g) ORCdial and chitosan reference spectra, (h) Chit-ORCdial composites with increasing ORCdial content; (i) Solid-state ^{13}C CP/MAS NMR spectra of ORCdial, chitosan, and Chit-ORCdial25 showing the imine carbon signal at ~165–170 ppm

The characterization by FTIR (Fig. 1g-h) confirmed the formation of covalent crosslinks between ORCdial and chitosan through Schiff base (aldimine) bond formation. In this reaction, the aldehyde groups (–CHO) of ORCdial could condense with the primary amine groups ($–NH_2$) of chitosan to form imine (C=N) bonds, releasing water.[21] This dialdehyde-amine crosslinking chemistry has been widely reported for cellulose-dialdehyde and chitosan systems.[19] In the FTIR spectra, a new absorption band appearing around 1640–1655 cm^{-1} was attributed to the C=N stretching vibration of the imine bond, confirming successful Schiff base formation. The intensity of this band increased progressively with increasing ORCdial content (Chit-ORCdial1 to Chit-ORCdial50), consistent with a higher degree of crosslinking at greater ORCdial ratio. Additionally, a reduction in the intensity of the primary amine

band (~1590 cm^{-1}, N-H bending of $–NH_2$) was observed relative to pure chitosan, indicating consumption of free amine groups during the crosslinking reaction.[21] The carboxylate stretching band of ORC (~1600 cm^{-1}) might partially overlap with the imine C=N region; however, the systematic shift and intensity changes observed as a function of ORCdial content supported the interpretation of covalent crosslink formation rather than mere physical blending (Fig. 1g-h). The Schiff base crosslinks in the final product were stabilized without the use of a chemical reducing agent (*e.g.*, sodium cyanoborohydride) through a combination of factors: (i) the multivalent nature of both ORCdial and chitosan produced a high crosslink density, providing collective kinetic stability to the network; (ii) the lyophilized matrix restricted polymer chain mobility, reducing the conformational freedom required for imine hydrolysis; and (iii) the alkaline pH established during NaOH neutralization suppressed protonation of the imine nitrogen, favoring the C=N bond stability. These stabilization mechanisms are consistent with the persistence of the C=N absorption band in the final processed product.

The Schiff base crosslinking was further investigated by solid-state ^{13}C CP/MAS NMR spectroscopy (Fig. 1i). Table 2 shows the summary of key evidence of crosslinking in Chit-ORCdial composites. In the spectrum of Chit-ORCdial25, a signal appearing in the ~165–170 ppm region was consistent with the resonance of imine carbon (C=N), which is the expected signature of Schiff base bond formation between an aldehyde and a primary amine. This chemical shift range is consistent with reported values for aldimine linkages in chitosan-based Schiff base networks (typically 158–170 ppm in solid-state ^{13}C NMR). This signal was absent or negligible in the spectra of pure chitosan and ORCdial, confirming that it arose specifically from the crosslinking reaction. The corrected NMR assignment (~165–170 ppm for the imine carbon) is fully consistent with the FTIR observation of the C=N stretching vibration at ~1640–1655 cm^{-1}, and both techniques independently confirm the formation of Schiff base bonds in the Chit-ORCdial25 composite. Furthermore, the C1 carbon of the anhydroglucose unit of ORCdial (~92–95 ppm) showed a downfield shift and broadening compared to unmodified ORC, which was consistent with the formation of hemiacetal or acetal structures under the reaction conditions. The relative intensities of the C4 (~80 ppm) and C6 (~60 ppm) carbons in the chitosan/ORCdial composite were also broadened, which could be attributed to restricted chain mobility resulting from the three-dimensional crosslinked network.[19] Only slight differences were observed in composites with low ORCdial content (*e.g.*, Chit-ORCdial1 and Chit-ORCdial5), which was expected given the low degree of crosslinking at these compositions (Fig. 1i).

Table 2
Summary of Schiff base crosslinking evidence in Chit-ORCdial composites

Technique	Signal/Band	Observed value	Assignment
FTIR	C=N stretching	~1640–1655 cm^{-1}	Imine bond
^{13}C CP/MAS NMR	Imine carbon	~165–170 ppm	–CH=N– (Schiff base)
^{13}C CP/MAS NMR	C1 carbon (ORCdial)	~92–95 ppm	Hemiacetal/acetal

Whole blood clotting time

Blood clotting studies were performed using recalcified citrated whole blood, which was an established model for comparing hemostatic activity *in vitro*.[20] The quantitative clotting times (mean ± SD) for all groups are presented in Figure 2.

The results demonstrated that ORCdial alone exhibited the weakest hemostatic performance among all groups ($p < 0.05$), consistent with its water-soluble, non-viscous nature, which limited its ability to physically entrap blood cells and initiate platelet plug formation in the absence of chitosan. The hemostatic activity increased with increasing ORCdial content in the composite structure. Chit-ORCdial25 and Chit-ORCdial50 achieved the highest hemostatic activity, with no statistically significant difference between these two groups ($p > 0.05$), indicating that 25% (w/w) ORCdial represented a threshold concentration beyond which additional ORCdial did not further improve clotting performance. This saturation effect was consistent with crosslink density theory: above a critical crosslink density, network pore size decreased to a point where red blood cell and platelet entrapment was no longer enhanced.[3,19] Chit-ORCdial1, Chit-ORCdial5, Chit-ORCdial10, and Celox® showed comparable coagulation performance ($p > 0.05$). The better performance of Chit-ORCdial25 over Celox®, combined with its improved biocompatibility profile, made it a more favourable

hemostatic candidate. The mechanism by which the composite accelerated clotting was likely multifactorial: (i) the cationic surface of chitosan electrostatically might interact with the negatively charged phospholipid membranes of erythrocytes and platelets, triggering aggregation;[9,22] (ii) ORCdial might absorb water from blood, concentrating clotting factors at the wound site;[13,14] and (iii) the three-dimensional crosslinked particle network could provide a physical scaffold for fibrin deposition and thrombus stabilization.[3,23]

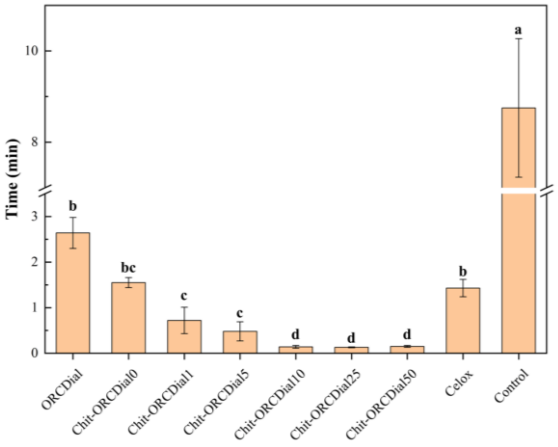

Figure 2: Whole blood clotting time of hemostatic materials (control = without hemostatic material; [a-c] different letters indicate statistically significant differences ($p < 0.05$))

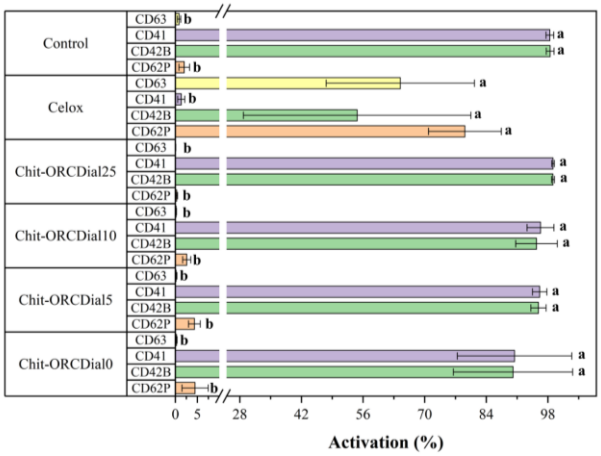

Figure 3: Platelet-leukocyte aggregate formation induced by hemostatic materials ([a-b] different letters indicate statistically significant differences ($p < 0.05$))

Platelet activation

Platelet activation and degranulation are essential components of the clotting process, thus, *in vitro* platelet activation studies were performed to understand the clotting mechanisms of materials. Flow cytometry is a commonly used method for evaluating platelet reactivity by assessing the expression levels of activation-dependent surface markers, as well as leukocyte-platelet aggregation.[24] The GPIIb/IIIa complex, also known as CD41/CD61 in CD nomenclature, is a heterodimeric structure consisting of a heavy α (IIb) and a light β (IIIa) chain linked by a disulfide bond[25] and is widely used as a platelet identification marker. Activation causes platelets to express P-selectin (CD62P), which facilitates binding between platelets and other cell types.[26–28] The increasing platelet-level activation of CD62P is one of the markers of platelet activation under in vitro conditions.[24] Glycoprotein (GP) Ib, also known as CD42bα, is located on the cell surface and forms a complex with factor IX, factor V and von Willebrand factor (vWF). The formation of this complex causes CD42b on the platelet surface to decrease, a phenomenon known as ectodomain shedding.[29] CD42bα secretion after platelet activation increases the stability of the resulting platelets and their interaction with CD62P.[29] CD63, a lysosomal antigen expressed on the platelet surface, can also be observed after platelet activation.[30] CD63 modulates platelet attachment to fibrinogen and spreading,[31] and its expression is a strong indicator of platelet activation.[32] Activated platelets also interact with leukocytes[33] via CD62 present on platelets, as well as various molecules expressed by leukocytes, such as PSGL-1, CD40 and Mac-1 to form platelet-leukocyte aggregates. These interactions induce the activation and release of granular content of both cell types, and play a role in the recruitment of leukocytes to inflammation sites to induce inflammatory responses. Thus, these activities were tested to evaluate the biocompatibility and hemostatic efficacy necessary for stable clot formation, as shown in Figures 3 and 4.

In the present study, it was observed that the formation of platelet-leukoaggregates induced by Celox® was significantly different from the control group ($p<0.05$), in contrast to the Chit-ORCdial0, ORCdial and Chit-ORCdial25 groups (Fig. 3). Besides, when comparing the other hemostatic agents except Celox®, there was no significant difference among control, Chit-ORCDial25, and Chit-ORCdial0. However, the expression of CD41 was significantly lower than those for both the control and the other test groups ($p<0.05$), which might suggest the presence of platelet death.[34] While activated platelets play a crucial role in thrombus formation, there is accumulating evidence suggesting the presence of different subpopulations of platelets during the coagulation cascade.[35] One

such subset is the “procoagulant platelets”, which can promote thrombin burst to provide thrombus stability.[36] However, procoagulant platelets have been reported to exhibit morphological features similar to necrosis under both electron and phase contrast microscopy. In addition, a combination of the cell death marker 4-[N-(S-glutathionylacetyl) amino] phenylarsonous acid and CD62P has been previously used to identify procoagulant platelets.[34] As a result, the application of Celox® led to lysis of the procoagulant platelets, releasing thrombus and decreasing the CD41 level, making further analysis impossible due to the low number of remaining cells. These results might explain the low platelet rate due to cell death induced by Celox® application, and therefore, it was excluded when comparing platelet activation according to platelet surface markers.

Flow cytometric analysis of platelet surface markers revealed mechanistically important differences between the test groups, as shown in Figure 4.

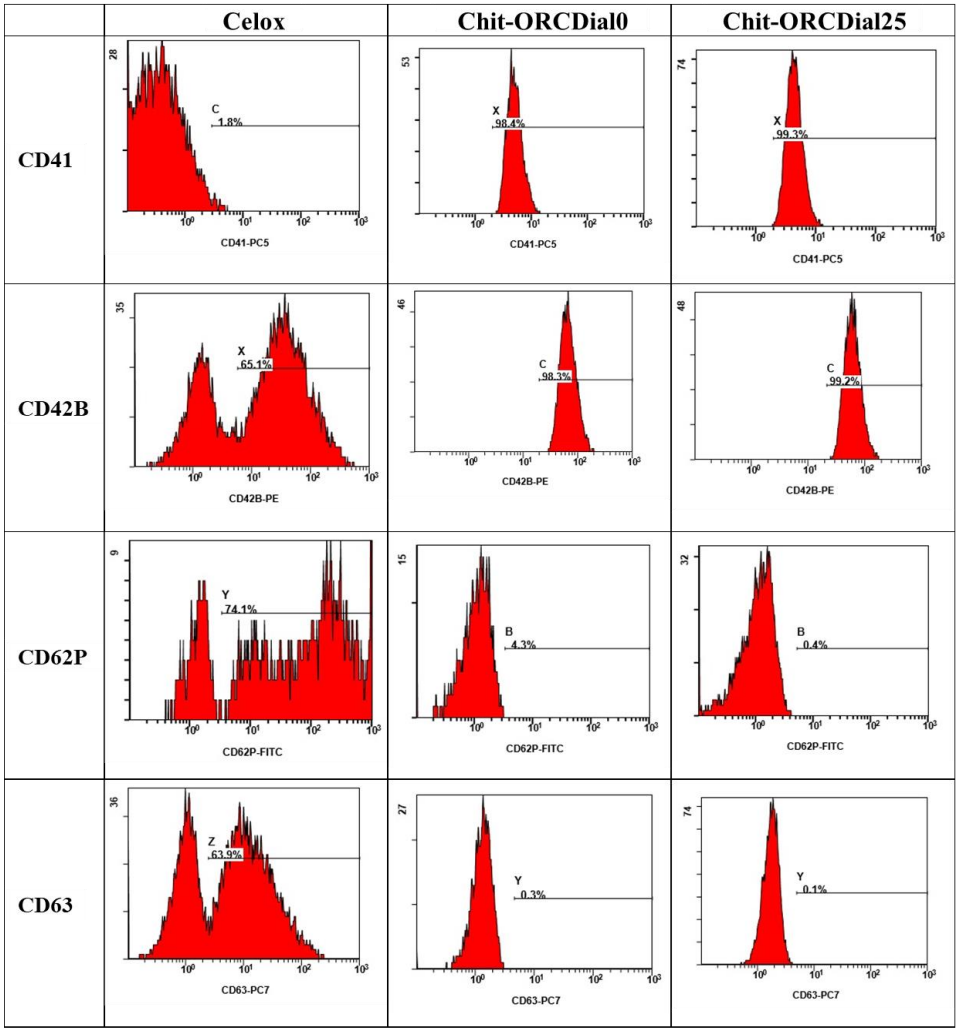

Figure 4: Flow cytometry histograms of platelet activation markers after incubation with ORCdial, Chit-ORCdial0, and Chit-ORCdial25; Untreated whole blood served as control

The levels of CD41 showed no significant difference between the Chit-ORCdial0, ORCdial, and Chit-ORCdial25 groups and the control group ($p>0.05$). Similarly, no differences in CD42b levels were observed between the treatment and control groups ($p>0.05$). The Celox® group exhibited significantly elevated CD62P (P-selectin) and CD63 expression compared to all other groups ($p < 0.05$), indicative of strong alpha-granule and dense-granule release, respectively.[26,32] P-selectin surface expression is a recognised marker of platelet activation and is associated with the formation of platelet-leukocyte aggregates that can amplify local inflammation at the wound site.[26,33] The observation that Celox® induced significantly higher platelet-leukocyte aggregate formation compared to all other groups ($p < 0.05$) was consistent with its strong charge-mediated platelet activation

mechanism and was in agreement with reports describing pro-inflammatory side effects of highly charged chitosan formulations.[11,22] In contrast, no significant differences in CD62P, CD63, CD41 or CD42b expression were detected among the Chit-ORCdial0, ORCdial, Chit-ORCdial25 and control groups ($p > 0.05$), suggesting that these materials did not induce non-physiological platelet activation under *in vitro* conditions. The near-normal CD42b (GPIbα) levels in the Chit-ORCdial25 group were particularly noteworthy: decreased CD42b was a marker of ectodomain shedding associated with shear-induced or drug-induced platelet injury,[29,37] and its maintenance at control levels indicated that Chit-ORCdial25 did not compromise platelet membrane integrity at the doses tested. The notably reduced CD41 levels observed in the Celox® group might be attributed to lysis of procoagulant platelet subpopulations, consistent with the necrosis-like morphology described for highly activated procoagulant platelets,[34,35] and were further evidence of the disruptive interaction of Celox® with platelet populations at the concentrations used in this study.

In-vitro cell studies

The safety of a hemostatic agent is an important issue for clinical practice.[38] Thus, the biocompatibility of the materials was evaluated using complementary cytotoxicity assays at different time points to capture both acute and intermediate cell responses. As shown in Figure 5, at 6, 12, and 24 h post-exposure (MTT assay), Chit-ORCdial25 and the pure chitosan control (Chit-ORCdial0) had the highest proliferative signal, consistent with the known mitogenic and cytoprotective effects of chitosan on endothelial cells.[4,9] The ORCDial group was statistically different from all groups, except Celox.

The time-dependent decrease in MTT absorbance observed in the ORCdial group was noteworthy: ORCdial, when dissolved alone, released short-chain aldehyde-bearing oligomers that might exert cytotoxic effects through carbonyl-mediated protein cross-linking and oxidative stress at extended incubation times.[13,23] However, when ORCdial was covalently incorporated into the chitosan network, aldehyde groups might be consumed in imine bond formation, rendering them unavailable for cellular interactions. This effectively might stop the cytotoxicity associated with free aldehyde groups, explaining the significantly improved cell viability of Chit-ORCdial composites relative to ORCdial alone. This mechanism of toxicity mitigation through covalent sequestration of reactive aldehyde groups has been described for other dialdehyde-polysaccharide systems.[19] The increase in Celox® cytotoxicity between 6 and 12 h was consistent with accumulating membrane disruption by the highly cationic chitosan in Celox®, which might be attributed to destabilisation of cell membrane phospholipid bilayers at higher concentrations and longer contact times.[11,22] These findings could support the better short-term biocompatibility profile of Chit-ORCdial25 relative to the commercial comparator.

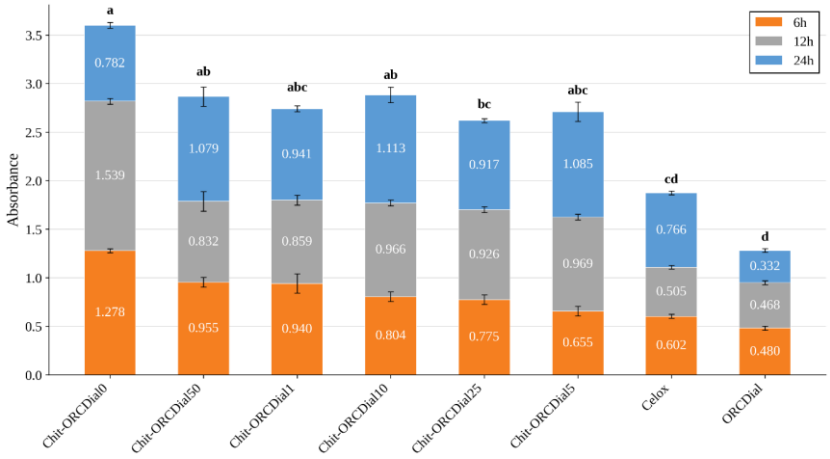

Figure 5: MTT cytotoxicity assay of hemostatic materials on HUVEC cells at 6, 12, and 24 h; Different letters indicate statistically significant differences ($p < 0.05$)

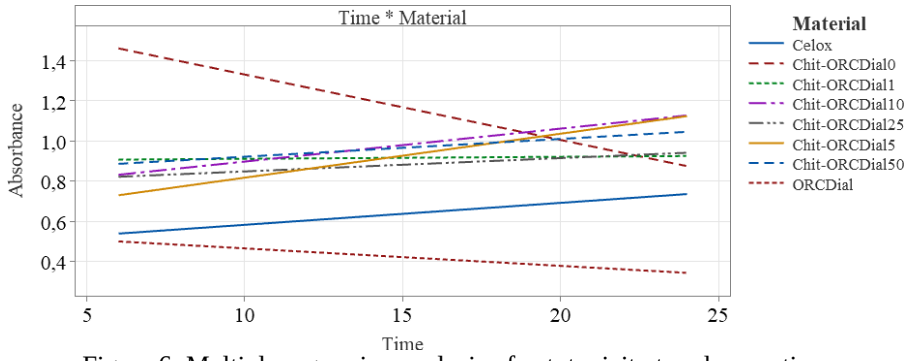

Figure 6: Multiple regression analysis of cytotoxicity trends over time

When the multiple regression results for all these materials were examined (Fig. 6), it was seen that the cytotoxicity in the ORCDial group and the Chit-ORCDial0 group decreased over time, while the cytotoxicity value increased over time in the other groups. While the time-dependent increase in cytotoxicity values was highest in the Chit-ORCDial5 group, the least increase was in the Chit-ORCDial50 group. This is in agreement with ORCDial, which has the lowest absorbance value.

Fluorescence imaging

According to the results obtained in MTT assay, it was expected that the materials could reduce cell viability by creating a negative effect on cell viability over time. To examine this situation, the live-dead assay was performed with the hemostatic materials and without hemostatic materials as a control group, as shown in Figure 7.

The live/dead fluorescence assay, performed at 72 h, demonstrated that all Chit-ORCdial composite groups supported HUVEC viability above 90%, with Chit-ORCdial25 yielding the highest viability of 95.67% and Chit-ORCdial0 reaching 95.19% (Table 3). Notably, cell viability in all composite groups exceeded that of the untreated control group (78.13%), which could be interpreted as a reflection of the cell-proliferative properties of chitosan and ORCdial rather than an artefact. This observation was consistent with the well-documented pro-proliferative and wound-healing-supportive properties of chitosan, which promoting cell adhesion, migration, and proliferation through interactions with cell-surface proteoglycans and growth factor receptors.[4,9]

The relatively lower viability in the untreated control group at 72 h might reflect contact-inhibition effects in confluent monolayers, a phenomenon commonly observed in endothelial cell cultures at high density without mitogenic stimulation.[11] In contrast, the powder materials might disrupt monolayer confluence and thereby re-stimulate proliferative signalling, as has been reported for polysaccharide-based biomaterials interacting with endothelial cells.[10,19]

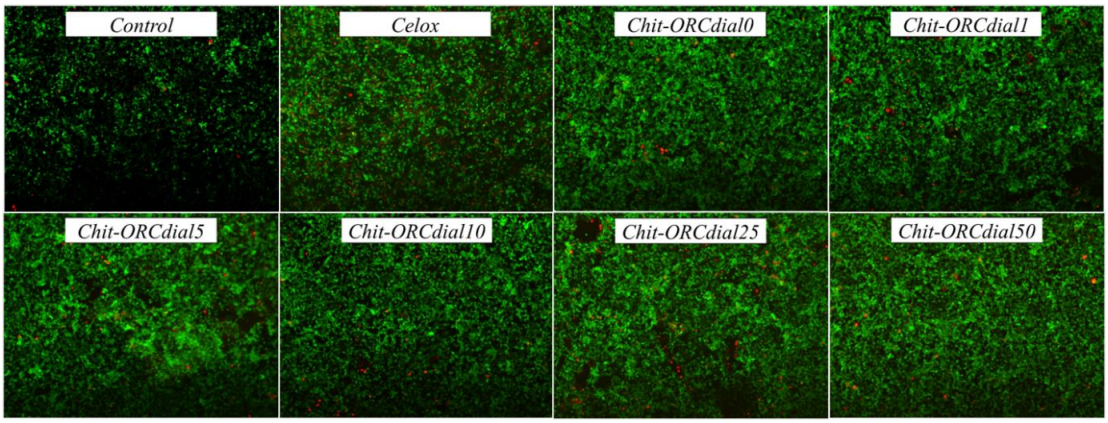

Figure 7: Live/Dead fluorescence viability assay of HUVECs after 72 h incubation with hemostatic materials

Table 3
Live/dead assay results of the hemostatic materials

Hemostatic materials	Live	Dead	Total	%Live
Celox	6102	3022	9124	66.88
Chit-ORCdial0	4095	207	4302	95.19
Chit-ORCdial1	4285	266	4551	94.16
Chit-ORCdial5	2881	271	3152	91.40
Chit-ORCdial10	4345	343	4688	92.68
Chit-ORCdial25	4195	190	4385	95.67
Chit-ORCdial50	4668	287	4955	94.21
Control	4759	1332	6091	78.13

The difference in time points between the MTT assay (6 and 12 h) and the live/dead assay (72 h) was intentional: the MTT assay was designed to capture early acute cytotoxic responses, whereas the live/dead assay was conducted at 72 h to allow sufficient cell-material interaction time and to reflect longer-term biocompatibility, consistent with approaches reported in the literature for hemostatic powder biocompatibility assessments.[3,11] The Celox® group showed a viability of only 66.88%, falling below even the untreated control group. This finding aligned with previous reports, indicating cytotoxic effects of chitosan-based commercial products under *in vitro* conditions, attributed to the high charge density and membrane-disrupting activity of the highly deacetylated chitosan formulation used in Celox®.[22] The acidic microenvironment generated by Celox® upon dissolution might further contribute to reduced cell viability, as sustained pH reduction in culture medium has been shown to impair endothelial cell function.[15]

CONCLUSION

In conclusion, this study presented the first synthesis and hemostatic evaluation of ORCdial-crosslinked chitosan composite particles, in which ORCdial served the dual role of a hemostatic agent and a covalent crosslinker via Schiff base bond formation with chitosan. The crosslinking was evidenced by FTIR (C=N band at ~1640–1655 cm^{-1}) and ^{13}C CP/MAS NMR spectroscopy (imine carbon at ~165–170 ppm). Among the compositions evaluated, Chit-ORCdial25 was the optimal formulation, exhibiting both the highest hemostatic activity (equivalent to Chit-ORCdial50, $p > 0.05$) and better biocompatibility relative to Celox® in HUVEC cell culture and platelet activation assays. The threshold effect at 25% ORCdial content could provide a practically important point for future formulation development. The elimination of cytotoxic free aldehyde groups through covalent crosslinking might represent a key safety advantage of the composite approach over ORCdial used alone. These results could support the potential of Chit-ORCdial25 as a biocompatible and effective candidate hemostatic material, which might also offer biodegradability advantages pending further investigation. However, the present study is limited to *in vitro* evaluation; further pre-clinical studies in appropriate animal models are necessary to validate hemostatic efficacy, tissue biocompatibility, and biodegradation kinetics under physiological conditions before clinical translation can be considered.

ACKNOWLEDGEMENT: We gratefully acknowledge the financial support of the Scientific and Technological Research Council of Turkey (TUBITAK) by its Technology and Innovation Funding Programmes Directorate (TEYDEB) foundation (Project number: 7190492) and Suleyman Demirel University BAP (Project Number: TSG-2018-6749). The authors declare no conflict of interest.

REFERENCES

[1] D. A. Hickman, C. L. Pawlowski, U. D. S. Sekhon, J. Marks and A. Sen Gupta, *Adv. Mater.*, **30**, 1700859 (2018), https://doi.org/10.1002/adma.201700859

[2] X. Wang, Q. Liu, J. Sui, S. Ramakrishna, M. Yu *et al.*, *Adv. Healthc. Mater.*, **8**, 1 (2019), https://doi.org/10.1002/adhm.201900823

[3] S. Liu, Z. Zheng, S. Wang, S. Chen, J. Ma *et al.*, *Carbohyd. Polym.* **224**, 115175 (2019), https://doi.org/10.1016/j.carbpol.2019.115175

[4] Y. Huang, L. Feng, Y. Zhang, L. He, C. Wang *et al.*, *Polym. Adv. Technol.*, **28**, 1107 (2017), https://doi.org/10.1002/pat.4003

[5] A. Chaturvedi, M. B. Dowling, J. P. Gustin, T. M. Scalea, S. R. Raghavan *et al*., *J. Surg. Res*., **207**, 45 (2017), https://doi.org/10.1016/j.jss.2016.04.052
[6] Q. Chen, Y. Liu, T. Wang, J. Wu, X. Zhai *et al*., *J. Mater. Chem. B*, **5**, 3686 (2017), https://doi.org/10.1039/c7tb00032d
[7] D. Li, P. Li, J. Zang and J. Liu, *J. Biomed. Biotechnol*., **981321**, 1 (2012), https://doi.org/10.1155/2012/981321
[8] J. Shen, A. A. Nada, N. Y. Abou-Zeid and S. M. Hudson, *Carbohyd. Polym*., **229**, 115522 (2020), https://doi.org/10.1016/j.carbpol.2019.115522
[9] G. M. Seon, M. H. Lee, B.-J. Kwon, M. S. Kim, M.-A. Koo *et al*., *Acta Biomater*., **48**, 175 (2017), https://doi.org/10.1016/j.actbio.2016.10.024
[10] X. Sun, Z. Tang, M. Pan, Z. Wang, H. Yang *et al*., *Carbohyd. Polym*., **177**, 135 (2017), https://doi.org/10.1016/j.carbpol.2017.08.131
[11] S. Pourshahrestani, E. Zeimaran, N. A. Kadri, N. Gargiulo, H. M. Jindal *et al*., *ACS Appl. Mater. Interfaces*, **9**, 31381 (2017), https://doi.org/10.1021/acsami.7b07769
[12] U. A. Sezer, Z. Kocer, İ. Sahin, B. Aru, G. Y. Demirel *et al*., *Carbohyd. Polym*., **200**, 624 (2018), https://doi.org/10.1016/j.carbpol.2018.07.074
[13] S. Zhang, J. Li, S. Chen, X. Zhang, J. Ma *et al*., *Carbohyd. Polym*., **230**, 115585 (2020), https://doi.org/10.1016/j.carbpol.2019.115585
[14] W. Cheng, J. He, Y. Wu, C. Song, S. Xie *et al*., *Cellulose*, **20**, 2547 (2013), https://doi.org/10.1007/s10570-013-0005-5
[15] M. U. Wagenhäuser, J. Mulorz, W. Ibing, F. Simon, J. M. Spin *et al*., *Sci. Rep*., **6**, 32238 (2016), https://doi.org/10.1038/srep32238
[16] F. Cheng, J. He, T. Yan, C. Liu, X. Wei *et al*., *RSC Adv*., **6**, 94429 (2016), https://doi.org/10.1039/c6ra15983d
[17] J. M. He, Y. D. Wu, F. W. Wang, W. L. Cheng, Y. D. Huang *et al*., *Fibers Polym*., **15**, 504 (2014), https://doi.org/10.1007/s12221-014-0504-5
[18] Z. Basagaoglu Demirekin, U. Aydemir Sezer, D. Ulusoy Karatopuk and S. Sezer, *Ind. Eng. Chem. Res*., **54**, 4906 (2015), https://doi.org/10.1021/ie504985b
[19] S. S. Biranje, J. Sun, Y. Shi, S. Yu, H. Jiao *et al*., *Cellulose*, **28**, 8899 (2021), https://doi.org/10.1007/s10570-021-04132-x
[20] A. K. Gaharwar, R. K. Avery, A. Assmann, A. Paul, G. H. McKinley *et al*., *ACS Nano*, **8**, 9833 (2014), https://doi.org/10.1021/nn503719n
[21] M. Dash, F. Chiellini, R. M. Ottenbrite and E. Chiellini, *Prog. Polym. Sci*., **36**, 981 (2011), https://doi.org/10.1016/j.progpolymsci.2011.02.001
[22] M. H. Periayah, A. S. Halim, A. R. Hussein, A. Z. Mat Saad, A. H. Abdul Rashid *et al*., *Int. J. Biol. Macromol*., **52**, 244 (2013), https://doi.org/10.1016/j.ijbiomac.2012.10.001
[23] A. M. Behrens, M. J. Sikorski, T. Li, Z. J. Wu, B. P. Griffith *et al*., *Acta Biomater*., **10**, 701 (2014), https://doi.org/10.1016/j.actbio.2013.10.029
[24] J. Curvers, J. De Wildt-Eggen, J. Heeremans, J. Scharenberg, D. De Korte *et al*., *Transfusion* (*Paris*), **48**, 1439 (2008), https://doi.org/10.1111/j.1537-2995.2008.01738.x
[25] A. Duperray, A. Troesch, R. Berthier, E. Chagnon, P. Frachet *et al*., *Blood*, **74**, 1603 (1989), https://doi.org/10.1182/blood.V74.5.1603.1603
[26] C. N. Jenne, R. Urrutia and P. Kubes, *Int. J. Lab. Hematol*., **35**, 254 (2013), https://doi.org/10.1111/ijlh.12084
[27] M. C. Berndt, P. Metharom and R. K. Andrews, *Haemophilia*, **20**, 15 (2014), https://doi.org/10.1111/hae.12427
[28] A. S. Weyrich, "Hematology 2014", the American Society of Hematology Education Program Book, 2014, pp. 400–403, https://doi.org/10.1182/asheducation-2014.1.400
[29] J. Hu, N. K. Mondal, E. N. Sorensen, L. Cai, H.-B. Fang *et al*., *J. Heart Lung Transplant*., **33**, 71 (2014), https://doi.org/10.1016/j.healun.2013.08.013
[30] M. J. Metzelaar, P. L. Wijngaard, P. J. Peters, J. J. Sixma, H. K. Nieuwenhuis *et al*., *J. Biol. Chem*., **266**, 3239 (1991), https://doi.org/10.1016/S0021-9258(18)49980-2
[31] S. J. Israels and E. M. McMillan-Ward, *Thromb. Haemost*., **93**, 311 (2005), https://doi.org/10.1160/TH04-08-0503
[32] K. J. Clemetson and J. M. Clemetson, in "Platelets", edited by A. D. Michelson, Elsevier, 2019, pp. 169–192, https://doi.org/10.1016/B978-0-12-813456-6.00009-6
[33] W. C. Schrottmaier, J. B. Kral, S. Badrnya and A. Assinger, *Thromb. Haemost*., **114**, 478 (2015), https://doi.org/10.1160/TH14-11-0943
[34] V. M. Hua, L. Abeynaike, E. Glaros, H. Campbell, L. Pasalic *et al*., *Blood*, **126**, 2852 (2015), https://doi.org/10.1182/blood-2015-08-663005

[35] J. W. M. Heemskerk, N. J. A. Mattheij and J. Cosemans, *J. Thromb. Haemost.*, **11**, 2 (2013), https://doi.org/10.1111/jth.12045
[36] S.P. Jackson, *Nat. Med.* **17**, 1423 (2011), https://doi.org/10.1038/nm.2515
[37] Y. Tao, X. Zhang, X. Liang, J. Zang, X. Mo *et al.*, *Sci. Rep.*, **6**, 24789 (2016), https://doi.org/10.1038/srep24789
[38] Q. Ouyang, T. Hou, C. Li, Z. Hu, L. Liang *et al.*, *Int. J. Biol. Macromol.*, **139**, 719 (2019), https://doi.org/10.1016/j.ijbiomac.2019.07.163